Clays Clay Miner., Vol. 70, No. 2:290–304, 2022
https://doi.org/10.1007/s42860-022-00186-5

LETTER

Sodium Polyacrylate-Modified Bentonite and Its Dehydration Testing in Real Oil

Fanyu Meng · Li Shi · Xuan Meng · Naiwang Liu

Accepted: 17 May 2022

Abstract Removing trace water from oil is an important industrial process and is commonly accomplished using vacuum filtration. The drawbacks of this method, however, are: poor efficiency, large oil loss, and significant energy consumption. The objective of the current study was to develop a better system to solve these problems using a sodium polyacrylate (PAA-Na)-modified bentonite as the dehydrating agent and, for the first time, to apply it to transformer oil. PAA-Na was prepared by aqueous solution polymerization. A dehydration test was carried out to determine the optimum addition of PAA-Na, and the highest dehydration rate of 76.5% was obtained with the addition of 20 wt.% PAA-Na. The steady dehydration rate of the PAA-Na-modified bentonite was better than that of other adsorbents (calcium chloride, zeolite 5A, unmodified bentonite). The process of adsorbing saturated water vapor on PAA-Na modified bentonite was studied and interpreted from the aspects of adsorption isotherms and thermodynamic properties. The results showed that the adsorption isotherm data followed the Freundlich isotherm model and the thermodynamic parameters indicated that the process was endothermic. Fourier-transform infrared spectroscopy results revealed that PAA-Na was synthesized successfully and it had a huge proportion of hydrophilic groups. According to thermogravimetric analysis, the PAA-Na-modified bentonite was stable up to 200°C, giving a flexible region for pretreatment and regeneration. X-ray diffraction showed no change in the diffraction pattern before and after modification. Moreover, considering the results of scanning electron microscopy and surface-area analyses, one may safely say that PAA-Na was distributed homogeneously on the surface of the bentonite. In addition, PAA-Na-modified bentonite exhibited a high dehydration rate in xylene, naphtha, and diesel, indicating a broad range of applications.

Keywords Adsorption · Bentonite · Dehydration · Freundlich isotherm model · Sodium polyacrylate · Trace-water removal · Transformer oil

F. Meng · L. Shi · X. Meng · N. Liu (✉)
State Key Laboratory of Chemical Engineering, East China University of Science and Technology, Shanghai 200237, China
e-mail: liunw@ecust.edu.cn

Introduction

Trace amounts of water contained in oil will significantly reduce the quality and life of the oil and might be a crucial contributor to system failure (Dechambre et al., 2017; Frink & Armstrong, 2016). For example, water in light fuel raises the freezing and crystallization points, causing low-temperature oil fluidity to deteriorate and clog the filter and oil path (Lam et al., 2013). Water in reforming feedstock oil can poison the catalyst (Moussa et al., 2018; Narayan et al., 2018). The current work was focused on the removal of trace water from transformer oil. A large moisture content leads to decrease in the dielectric strength and reduces drastically the breakdown voltage of transformer oil (Prakoso, 2015). Therefore, an efficient and in-line functional fast-action system to remove trace water in oil is needed urgently.

Traditional methods of oil/water separation are mechanical separation, including gravity sedimentation

(Powers, 1990), flotation (Saththasivam et al., 2016), hydrocyclone (Sheng et al., 1974), and so on. These separation methods have their advantages, but the disadvantages are also obvious: the gravity sedimentation method can remove only free water from oil with a low flow rate in a large-scale container (Spielman & Goren, 1970); the volume of the equipment used in the flotation method is large and consumes a large amount of energy (Xu et al., 2014); the hydrocyclone fails to separate the emulsified droplets with a particle size of <30 μm.

The dehydration object in this study is transformer oil with a water content of 30–40 ppm, and the goal was to reduce the water content to <10 ppm. The methods above are suitable only for dehydration when the oil contains a large amount of water, not for removal of trace amounts.

Other than the mechanical separation methods mentioned above, to remove trace moisture from oil products, chemical methods, membrane separation, and adsorption may be used. The adsorption process for oil/water separation has a number of benefits, including ease of operation, low energy consumption, and automated control. Traditional fixed-bed adsorbents are zeolites A, which rely on pore structure and diffusion for dehydration (Teo & Ruthven, 1986). It is impossible to avoid large amounts of oil adsorption, however. A novel adsorbent with a good dehydration effect for trace water in oils is needed.

To solve the problem of massive adsorption of transformer oil by zeolite A, a super adsorbent hydrogel sodium polyacrylate (PAA-Na) with hydrophilic and oleophobic properties was selected for study. Superadsorbent hydrogels are loosely crosslinked hydrophilic polymers that can adsorb, swell, and retain aqueous solutions up to hundreds of times their own weight (Santiago et al., 2007). PAA-Na has a large number of hydrophilic functional groups, which can form hydrogen bonds with trace amounts of water in the oil and has a significant dehydration depth.

PAA-Na is prone to swelling due to water adsorption, however. The main driving force for the swelling of PAA-Na is osmotic pressure, which is proportional to the concentration of ions in the aqueous solution. As the Na^+ ions are bounded by the polymer network, the osmotic pressure is very high. During water adsorption, the osmotic pressure is reduced by diluting the charges. The reset force of the polymer network and the external osmotic pressure work to offset this osmotic driving force. Other external pressures, e.g. if the PAA-Na has to swell or retain water against external mechanical forces, reduce the adsorption capacity as well. When all forces are equal, the swelling is in equilibrium (Ye et al., 2012). A large change in volume of PAA-Na will increase the fixed-bed pressure, which is unfavorable for industrial applications. It needs to be modified to limit its swelling. The expansion ratio of bentonite is far less than that of sodium polyacrylate. In the present study, therefore, bentonite was considered as a support to limit PAA-Na swelling by sequestering the water.

Because PAA-Na and bentonite both have significant water-adsorption capabilities, this study opted to combine the two to create a novel adsorbent. PAA-Na-modified clay has been the subject of numerous studies. PAA-Na enhanced significantly the adsorption performance of the modified bentonite by increasing the cation exchange capacity (Yu et al., 2019). The mechanical properties of Laponite were improved by modifying laponite with PAA-Na (Takeno & Nagai, 2018; Takeno & Nakamura, 2019). The aqueous dispersion of the synthetic saponite with PAA-Na formed a stable sol, compared to the synthetic saponite sol or synthetic saponite hydrogel (Li et al., 2019). Laponites could be transparent, self-standing, moldable, and robust hydrogels with shear-thinning and self-healing properties when sodium polyacrylate was added (Becher et al., 2019).

Transformer oil must be dehydrated before being fed into the transformer due to the fact that water will reduce the breakdown voltage of transformer oil. The vacuum filtration process is currently the most widely used technology in industry, although it has a number of drawbacks, including low efficiency, oil loss, and high energy consumption. The requirement is that the water content in transformer oil must be <10 ppm, especially in certain large high-voltage transformers. If the vacuum filtration technique is used to achieve this criterion, secondary filtration is required. In response to this circumstance, a new technique to replace vacuum filtration is required, which can remove water from transformer oil rapidly and efficiently, enhance oil quality, increase processing capacity, and simplify the process.

The main purpose of this research was to design a fixed-bed dehydration process for transformer oil and to develop a novel dehydration agent for the process. The hypothesis was that the dehydration of transformer oil can be accomplished using PAA-Na-modified bentonite and other adsorbents.

https://doi.org/10.1007/s42860-022-00186-5 Published online by Cambridge University Press

Experimental details

Materials

The bentonite used as the support was produced in Zhejiang, China, and consists mainly of Ca-montmorillonite which has a unit-cell formula, based on elemental analysis, of $Ca^{2+}_{0.41}(Si_{7.98}Al_{0.02})(Al_{3.00}Mg_{0.80}Fe^{3+}_{0.20})O_{20}(OH)_4$. The water layer is typically ~3.8–4.1 Å thick when Ca^{2+} is the exchangeable cation, given that the basal spacing is 14.2–14.5 Å (Murray, 2006).

The transformer oil for experiments in the laboratory was obtained from Gaoqiao Petrochemical Company of SINOPEC, Shanghai. The water content was ~10–40 ppm.

Preparation of Sodium Polyacrylate (PAA-Na)

Acrylic acid (Shanghai Macklin Biochemical Co., Ltd, Shanghai, China) and 20% NaOH (Shanghai Macklin Biochemical Co., Ltd, Shanghai, China) were used as raw materials, N,N-methylene bisacrylamide (CHEMBEE, Shanghai, China) was used as the crosslinking agent, and potassium persulfate was used as the initiator. PAA-Na was prepared by the aqueous solution polymerization method, as follows: 10 g of acrylic acid was added slowly to 40 mL of 20% NaOH solution in an ice-water bath for neutralization, and then 0.0195 g of initiator (potassium persulfate) and 0.03 g of crosslinking agent (N, N-methylene bisacrylamide) were added and stirred fully until dissolved. The solution was added to a flask equipped with a stirrer, condenser, and thermometer. The hydrogel was obtained after stirring on a magnetic heater in an 80°C water bath for 3 h. Finally, the hydrogel obtained was dried in a vacuum oven at 80°C for 24 h to obtain PAA-Na, and then the PAA-Na was ground into powder (>200 mesh) by hand with an agate mortar and pestle.

Preparation of Adsorbent

The bentonite adsorbent utilized in this study was prepared by kneading. To develop a series of modified bentonites, bentonite was mixed with various amounts of PAA-Na powder (10, 20, or 30 wt.%), then kneaded with a dough hook and mixer by adding water (30% of the mass of bentonite), and lastly squeezed into strips using a screw extruder (VanKood, Clay Sculpture Tool, Shenzhen, Guangdong, China).

The adsorbent was dried for 24 h at 80°C in an oven. Finally, the adsorbent was crushed and sieved. The 20–40 mesh particles were used for the dehydration test. The evaluation of the adsorbent in the laboratory was carried out in a fixed-bed microreactor equipped with a constant-flow pump to control the flow rate. Adsorbent was packed between two layers (each layer is 2 cm) of quartz sand (40–60 mesh) and inserted into the microreactor. The modified bentonite used in all experiments was 20 wt.% PAA-Na unless otherwise specified.

Water Content

The trace-water content of the transformer oil was measured every hour after dehydration using a Karl Fischer Titrator (MKC-710B, KEM, Kyoto, Japan). The dehydration rate, X%, was calculated using the following equation (Eq. 1):

$$X = (1 - C_i/C_0) \times 100 \quad (1)$$

where C_0 is the water content of the feedstock and C_i is the water content of the products. The adsorption process was performed at 25°C, atmospheric pressure, and a weight hourly space velocity of 8 h^{-1}. Weight hourly space velocity is defined as the weight of feed flowing per unit weight of the adsorbent per hour. It can determine the treatment capacity and operating conditions of adsorbents.

Adsorption Isotherm

The adsorption isotherms of water in the unmodified bentonite, 20 wt.% PAA-Na modified bentonite, and PAA-Na were studied at 10 and 25°C. The Freundlich and Langmuir models were used to describe the equilibrium characteristics as given by the following equations (Eqs 2, 3):

$$V = K_F \cdot (P/P_0)^{1/n} \quad (2)$$

$$V/(V_L - V) = K_L \cdot (P/P_0) \quad (3)$$

where V is volume adsorbed (cm^3/g), P is Presure (kPa), P_0 is the saturated vapor pressure of water at the corresponding temperature (kPa), K_F and n are Freundlich constants, K_L is the Langmuir constant.

https://doi.org/10.1007/s42860-022-00186-5 Published online by Cambridge University Press

Characterization

Fourier-transform infrared (FTIR) spectra were recorded using a Nicolet-6700 (Thermo Scientific, Waltham, Massachusetts, USA) FTIR spectrophotometer by mixing the sample with dried KBr and scanning at a resolution of 4 cm^{-1}. Thermogravimetric analysis (TGA) of the samples was carried out using a TA SDT Q600 instrument (TA Instruments, New Castle, Delaware, USA) by heating samples in the range 35–800°C at a heating rate of 10°C/min under air flow (30 cm^3/min). X-ray diffraction (XRD) of the representative samples (bentonite and PAA-Na-modified bentonites) was performed using a Rigaku-3016 (Rigaku, Akishima, Tokyo, Japan) instrument with CuKα radiation (λ = 0.154 nm), a generator voltage of 45 kV and a current of 25 mA, a step size of 0.02°2θ, and a scanning rate of 1°2θ/min from 3 to 50°2θ. Scanning electron microscopy (SEM) of the sample was carried out using a JEOL-JSM6301-F Electron Microscope (JEOL, Akishima, Tokyo, Japan) with an Oxford INCA/ENERGY-350 microanalysis system (Oxford Instruments, Abingdon, Oxfordshire, England). Surface area and average pore diameter of the samples were measured by N_2 adsorption-desorption using a JWGB-JQ200C (JEGB, Beijing, China) surface area analyzer. Samples were degassed under vacuum at 120°C for 2 h prior to the adsorption measurement to evacuate the adsorbed moisture. The surface area was calculated by the Brunauer-Emmett-Teller (BET) equation. Micropore volume-size distribution was calculated using the method of Horvath-Kawazoe (H-K) (Horváth & Kawazoe, 1983) and mesoporous volume-size distribution curve was calculated using the Barrett-Joyner-Halenda (BJH) method (Seaton et al., 1989) according to the adsorption branch.

Results and discussion

FTIR Spectra of Sodium Polyacrylate (PAA-Na)

The (FTIR) spectrum (Fig. 1a) of PAA-Na showed a characteristic peak at 3420 cm^{-1}, which was attributed to the hydroxyl stretching modes of the adsorbed water. The peaks appearing at 2926 and 2853 cm^{-1} were attributed to the methyl and methylene stretching vibrations. The peaks appearing at 1024 and 1411 cm^{-1} were attributed to the sulfonic and amide stretching vibrations. The peaks appearing at 1561 cm^{-1} were attributed to the asymmetric and symmetric stretching vibrations of the carboxylate anion. Moreover, the peak corresponding to the carbon-carbon double bond between 1620 and 1630 cm^{-1} disappeared, suggesting the carbon-carbon double bond was broken and participated in the reaction. The presence of these hydrophilic groups revealed by the infrared spectra proved the hydrophilicity of PAA-Na, and the appearance of the above characteristic peaks illustrated the successful synthesis of PAA-Na (Liu et al., 2021)

Water adsorption was monitored in situ using FTIR (Fig. 1b, 1c). The intensity of the hydroxyl stretching band of the bentonite and modified bentonite increased after water adsorption. The peak area in the range 3600–2500 cm^{-1} increased linearly with the amount of water adsorbed, by 13.97% in the unmodified bentonite and by 31.19% in the modified bentonite. The peak area of modified bentonite increased more because carboxyl creates a hydrogen bond with water in addition to hydroxyl.

Dehydration Test of Various Adsorbents

The PAA-Na powder swells several times its volume after water adsorption (Fig. 2), which increases the fixed-bed pressure and, thus, is not conducive to application in industrial oil dehydration. In contrast, after kneading with bentonite, the adsorbent volume did not change significantly after water adsorption. The stable physicochemical properties make PAA-Na-modified bentonite a good candidate for application in industrial oil dehydration. The steady dehydration rates of various adsorbents are shown in Table 1. Zeolite A is one material that is used extensively in industry to dehydrate water by physical adsorption. The channel diameter of the zeolite 5A is 0.5 nm, and the initial developmental intention of this material was that water molecules can enter its pore channel structure freely. Because the molecular size of oil is larger than the pore channel diameter, oil molecules cannot enter, so the pore volume of zeolite 5A can theoretically be occupied only by water molecules. The above characteristics of zeolite 5A can enhance the pore-volume utilization and avoid the competitive adsorption of oil and water. However, the actual dehydration effect for transformer oil does not reflect these advantages. This is because transformer oil has a higher viscosity than common reagents, e.g. benzene, toluene, and xylene, and its lack of fluidity at the orifice

https://doi.org/10.1007/s42860-022-00186-5 Published online by Cambridge University Press

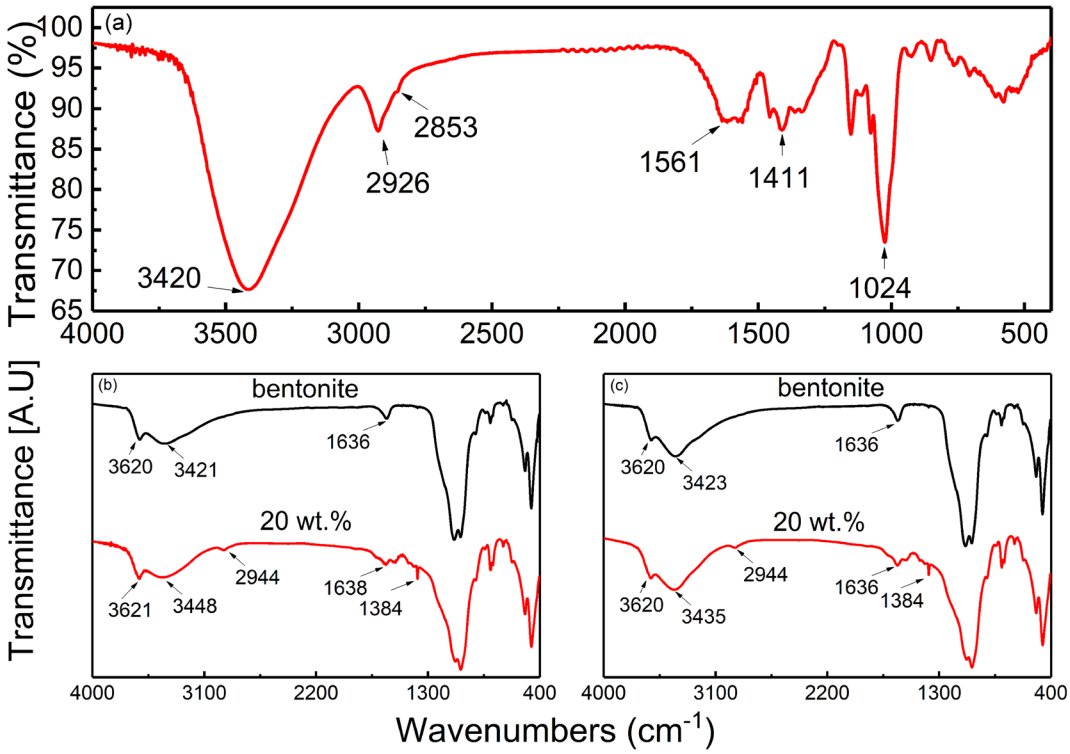

Fig. 1 **a** FTIR spectra of PAA-Na, FTIR spectra of bentonite and modified bentonite **b** before and **c** after water adsorption

of zeolite 5A micropores limits both the internal diffusion of water molecules and the process of water molecules entering the micropores to be adsorbed.

Anhydrous calcium chloride, a material commonly used in laboratories to achieve dehydration with the aid of chemisorption, is used commonly in organic synthesis. Although chloride ion loss is a problem when using calcium chloride in fixed-bed experiments, the goal here was to explore the depth of chemisorptive dehydration, in contrast to the zeolite 5A described above. According to the data in Table 1, the dehydration rate of anhydrous calcium chloride can reach 62%, which is greater than the 46% of zeolite 5A. The two main reasons for calcium chloride having a greater dehydration rate than zeolite 5A are: (1) during water adsorption by anhydrous calcium chloride, there is no diffusion resistance for water molecules because the adsorption-active sites of anhydrous calcium chloride are exposed to external surfaces directly; and (2) water adsorption by anhydrous calcium chloride is based on chemisorption, forming $CaCl_2{\cdot}6H_2O$ to absorb water molecules, and the force between calcium chloride and water molecules is stronger than the van der Waals force of physical adsorption or hydrogen bonding.

PAA-Na and calcium chloride both had a high selectivity for water adsorption in transformer oil. Water adsorption by PAA-Na is lower than calcium chloride because water adsorption by PAA-Na is a physical process, whereas calcium chloride water adsorption is a chemical reaction. The negative aspect of water removal from the oil by calcium chloride is that it introduces chloride ions into the oil, which affect the quality of the oil and corrode the metal equipment.

Bentonite is a good dehydrating agent, and the dehydration rate can reach 68.3%, according to Table 1. Most of the water is adsorbed as hydration water surrounding exchangeable cations in the interlayer region of smectites. Some additional water can be adsorbed by micro- or even mesopores. This additional water has been termed ‘external water’ (Kaufhold et al., 2010). These characteristics are responsible for the better water adsorption. As a result, the PAA-Na modified bentonite synthesized in the current work has a greater dehydration rate than other adsorbents because it combines the advantages of both PAA-Na and bentonite.

https://doi.org/10.1007/s42860-022-00186-5 Published online by Cambridge University Press

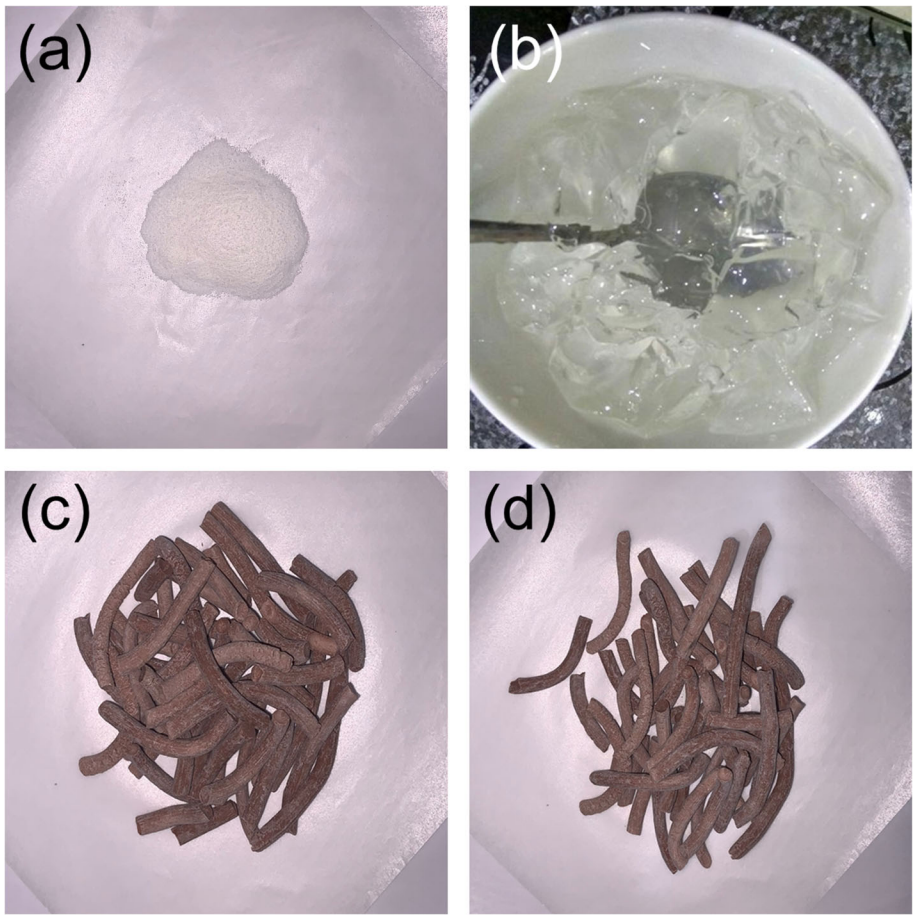

Fig. 2 PAA-Na powder **a** before and **b** after water adsorption; PAA-Na modified bentonite **c** before and **d** after water adsorption

Dehydration Test of PAA-Na-Modified Bentonites

A series of modified bentonites with various PAA-Na contents were prepared to test the effect of the PAA-Na additive. The water content of unprocessed transformer oil was 28 ppm. A steady dehydration rate of various modified bentonites are shown in Fig. 3a. The optimal amount of PAA-Na to modify the bentonite turned out to be 20 wt.%. When the addition of PAA-Na was <20 wt.%, the dehydration rate increased as the amount of PAA-Na added increased. When the addition was >20 wt.%, the dehydration rate decreased, indicating that the addition of PAA-Na will not increase the dehydration rate indefinitely and that an optimal value exists. At the same time, these observations proved that the water adsorption ability of modified bentonite depends on the joint action of PAA-Na and bentonite. PAA-Na contains abundant hydrophilic groups, so the addition of PAA-Na can improve the dehydration ability of bentonite, and the greater water content of the unprocessed transformer oil, the higher the dehydration rate (Fig. 3b).

Adsorption Isotherms

The water adsorption tests above were conducted using real oil, but did not reveal the water-adsorption process

Table 1 Steady dehydration rate of various adsorbents

Adsorbent	modified bentonite	bentonite	$CaCl_2$	Zeolite 5A	PAA-Na
Dehydration rate (%)	76.5	68.3	62.1	46.7	48.0

https://doi.org/10.1007/s42860-022-00186-5 Published online by Cambridge University Press

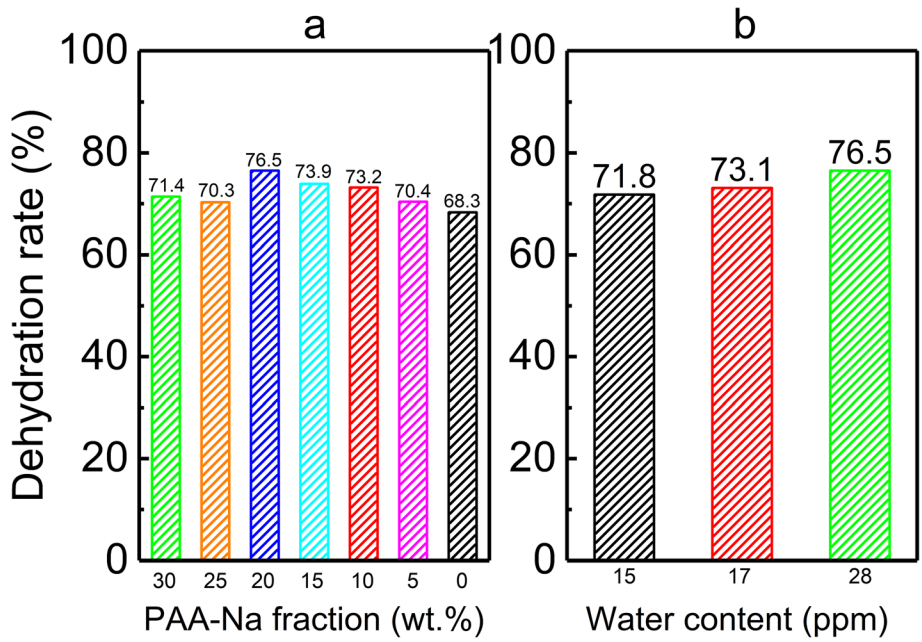

Fig. 3 **a** Steady dehydration rate of feed oil by bentonite modified with various amounts of PAA-Na; **b** steady dehydration rate of feed oil at various water contents using bentonite modified with 20 wt.% PAA-Na

in detail. To provide further understanding, experiments were undertaken with water concentrations ranging from 0 to 100%, with the expectation of gaining a broader view of water adsorption by modified bentonite.

Adsorption isotherms were obtained to provide information on adsorbate equilibrium relationships, affinities, and adsorption capacities of the adsorbents. Better recognition of the essential principles of adsorption and the parameters derived from the various equilibrium isotherm models could provide important information on the prediction of adsorption. Data were plotted according to the Freundlich isotherm model (Fig. 4), and the corresponding parameters and determination coefficient (R^2) (Tables 2 and 3) indicated that this model predicts well the adsorption of water vapor onto bentonite, PAA-Na, and modified bentonite (20 wt.%) under saturated water vapor conditions at 25 and 10°C. P_0 in Fig. 4 is the saturated vapor pressure of water at 25 and 10°C. The adsorption capacity and adsorption rate of bentonite improved after modification; PAA-Na modified bentonite exhibited a greater ability to entrap water molecules than bentonite due to the presence of hydrophilic groups, which was corroborated by the FTIR spectra (Fig. 1a). In the low relative pressure region ($P/P_0 < 0.45$), the modified bentonite had the highest water adsorption capacity. This finding is consistent with the results achieved by using modified bentonite to remove trace amounts of water from the oil. In the high relative-pressure region ($P/P_0 > 0.45$), the adsorption capacity of PAA-Na was greater than either the bentonite or modified bentonite, which is because the greater the external water content, the greater the osmotic pressure in the polymer framework of PAA-Na, thus causing the PAA-Na to adsorb more water.

Adsorption Thermodynamics

The adsorption process can also be described by adsorption thermodynamics. The state functions ΔS^{θ} (kJ/mol), ΔH^{θ} (kJ/mol), and ΔG^{θ} (kJ/mol) can be calculated from the following formulae (Saleem et al., 1992) (Eqs 4, 5):

$$\Delta G^{\theta} = -\mathrm{R}T\ln(\mathrm{K_C}) \tag{4}$$

$$\ln(\mathrm{K_C}) = \left(T\Delta S^{\theta} - \Delta H^{\theta}\right)/\mathrm{RT} \tag{5}$$

$$\mathrm{K_C} = \mathrm{K_F} \cdot \rho\left(10^6/\rho\right)^{(1-1/\mathrm{n})} \tag{6}$$

where $\mathrm{K_C}$ is the thermodynamic equilibrium constant without units (dimensionless) (Eq. 6), where

https://doi.org/10.1007/s42860-022-00186-5 Published online by Cambridge University Press

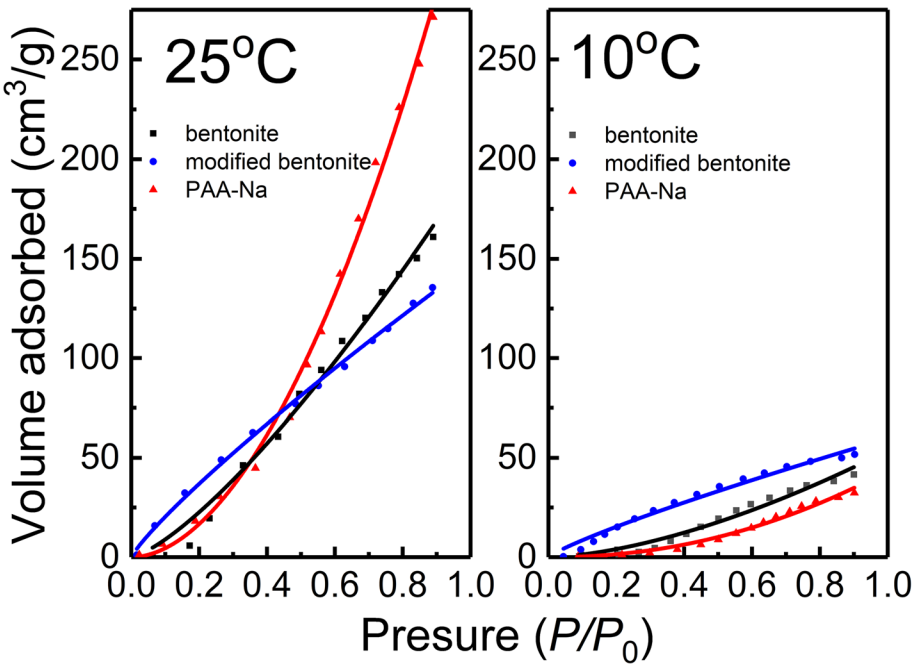

Fig. 4 Water-adsorption isotherms of bentonite, PAA-Na, and bentonite modified with 20 wt.% PAA-Na

ρ is the density of saturated water vapor at 20°C and 25°C (Ghosal & Gupta, 2015), R is the universal gas constant (8.314 $J{\cdot}mol^{-1}{\cdot}k^{-1}$); T is system temperature; and ΔH^{θ} and ΔS^{θ} were obtained from the slope and intercept of the relationship between K_C and $1/T$. The calculated results are listed in Table 4. The fact that the ΔG^{θ} value decreased as the temperature increased, as shown in Table 4, indicates that the process was thermodynamically favorable. The increased randomness throughout the adsorption process is indicated by the positive value of ΔS^{θ}. The positive ΔH^{θ} value indicated that the adsorption process was endothermic, which matches the adsorption isotherm result.

Table 2 Parameters derived from application of the Freundlich adsorption isotherm

Freundlich		Bentonite	Modified bentonite	PAA-Na
25°C	K_F	194.6	147.3	345.7
	1/n	1.337	0.8598	1.884
	R^2	0.9892	0.9975	0.9951
10°C	K_F	53.66	59.71	43.48
	1/n	1.602	0.8454	2.098
	R^2	0.9679	0.9811	0.9367

Thermal Stability Analysis

Thermogravimetric curves (Fig. 5) of bentonite and modified bentonite (20 wt.% PAA-Na) revealed that the weight loss due to adsorbed water occurred between 35 and 150°C for bentonite (Fig. 5a, DTG curve) and between 35 and 200°C for modified bentonite (Fig. 5b, DTG curve). Another weight loss was observed at ~200–500°C due to thermal decomposition of the PAA-Na polymer. The residual amount of modified bentonite was 76%, while that of bentonite was 85%, and the reduction of the residue was due to the decomposition of PAA-Na at high temperature.

Water molecules were removed between 35 and 200°C (Fig. 5), so drying temperatures of 80, 120, and 160°C were selected for pretreatment (Fig. 6). After 24 h of drying, the modified bentonite was used for trans-

Table 3 Parameters derived from application of the Langmuir adsorption isotherm

Langmuir		Bentonite	Modified bentonite	PAA-Na
25°C	K_L	0.00185	-6.206×10^{18}	-1.348×10^{19}
	R^2	0.9574	8.882×10^{-16}	–0.1818
10°C	K_L	2.5798×10^{-4}	4.798×10^{-4}	1.423×10^{-4}
	R^2	0.8755	0.8882	0.8160

https://doi.org/10.1007/s42860-022-00186-5 Published online by Cambridge University Press

Table 4 Thermodynamic parameters for bentonite, PAA-Na, and modified bentonite

	Bentonite	Modified bentonite	PAA-Na
ΔG^{θ} (25°C)	–3.714	–3.024	–5.139
ΔG^{θ}(10°C)	1.611	1.359	2.106
ΔH^{θ}	102.1	84.10	138.9
ΔS^{θ}	0.3550	0.2922	0.4830

former oil dehydration at 25°C and atmospheric pressure with a weight hourly space velocity of 8 h^{-1}. The dehydration curves of modified bentonite pretreated at 80 and 160°C were similar. The modified bentonite pretreated at 120°C showed the best dehydration effect. The pretreatment temperature of the modified bentonite, therefore, was selected as 120°C.

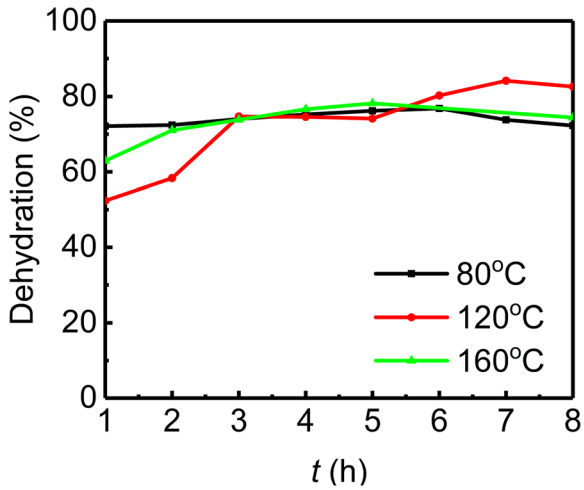

Fig. 6 Steady dehydration rate at various drying temperatures of bentonite modified with 20 wt.% PAA-Na

Influence of Weight Hourly Space Velocity

The space velocity is an important parameter in the adsorption experiment for modified bentonite (20 wt.% PAA-Na); under various space velocities (ranging from 8 to 60 h^{-1}), the extent of water adsorption was largely consistent, and ultimately reached ~80% (Fig. 7). Operating conditions, therefore, can be changed flexibly in industrial applications. Modified bentonite can maintain a stable dehydration rate even when the space velocity fluctuates significantly. At a space velocity of 30 h^{-1}, each gram of adsorbent can treat 4750 g of transformer oil and each gram of adsorbent can adsorb 139.3 mg of water from oil.

Transformer Oil Quality Index after Dehydration

PAA-Na modified bentonite was developed as an adsorbent specifically for dehydration, and the trace water

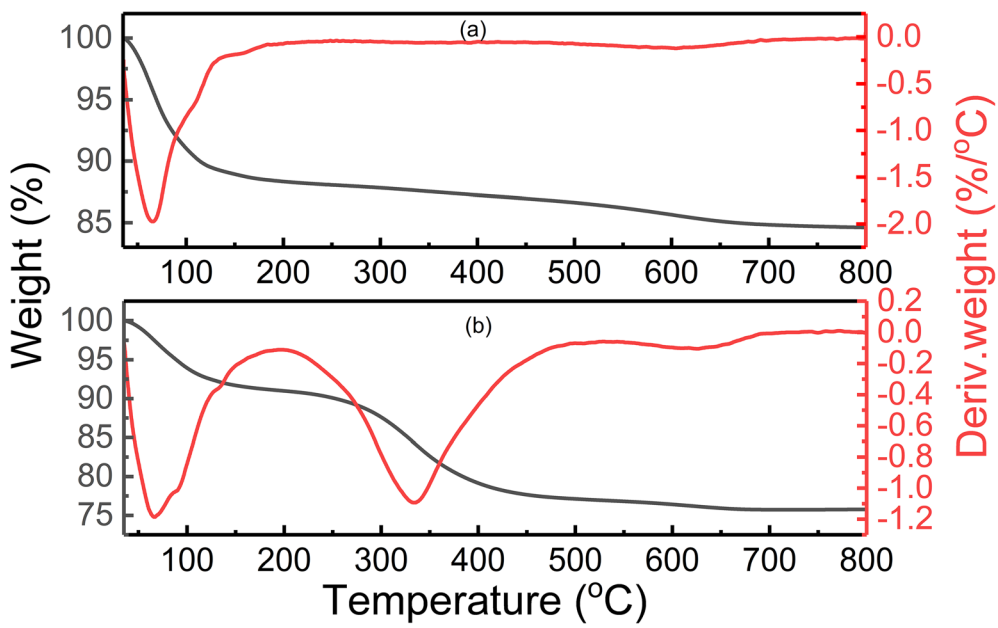

Fig. 5 TGA curves of **a** bentonite and **b** bentonite modified with 20 wt.% PAA-Na

https://doi.org/10.1007/s42860-022-00186-5 Published online by Cambridge University Press

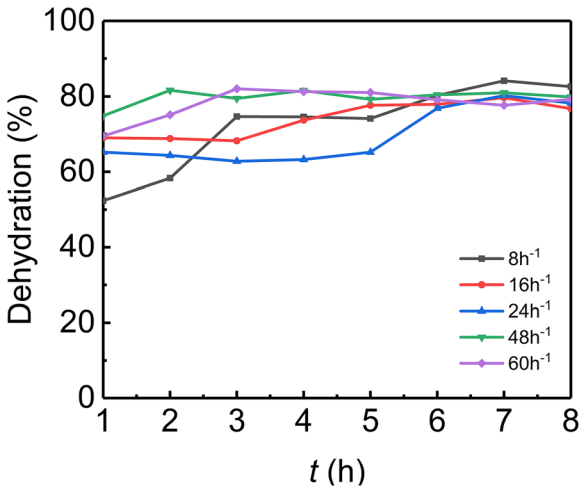

Fig. 7 Steady dehydration rate of feed oil containing 28 ppm water at various space velocities

in transformer oil should be removed selectively without reducing the quality of the transformer oil. In order to assess changes in quality indicators of transformer oil before and after treatment with modified bentonite, a series of tests was carried out (Table 5). After examination and comparison of oil quality indicators before and after dehydration, modified bentonite was shown to be effective at trace-water removal from transformer oil and the breakdown voltage was also improved. Modified bentonite also reduced kinematic viscosity and dielectric loss factor; it may be that the modified bentonite also adsorbs other components from the oil, thereby further improving its performance.

Analysis of Morphology

X-ray diffraction was used to analyze the mineral composition and crystal structure (Park et al., 2011). Figure 8 shows the XRD patterns of bentonite and PAA-Na-modified bentonite before and after water adsorption. The patterns are very similar, which suggests that the PAA-Na did not intercalate into the interlayer spaces of the bentonite. The interlayer distance should increase and the d_{001} spacing should decrease if PAA-Na was intercalated into the interlayer (Natkański et al., 2012), but such changes were not observed, as reported in the literature (Guerra et al., 2008). The several sharp diffraction peaks of the five samples were due to a large amount of silica (Kawi & Yao, 1999) in the bentonite. Comparing the micro morphologies of bentonite and modified bentonite (20 wt.%) in Fig. 9, showed that the layers of both bentonites remained relatively intact, the edges appeared curled, and the crystal form was not destroyed, consistent with the conclusions from XRD. After PAA-Na modification, the bentonite layers became more compact, and the granular protrusion was significantly reduced.

BET Analysis

The pore structures of the bentonite and the modified bentonites were investigated by N_2 adsorption-desorption isotherms (Fig. 10). Isotherms of both bentonite and modified bentonites are type IV

Table 5 Transformer oil quality index before and after dehydration

Analysis type	Quality indicator	Before processing	After processing	Test method
Pour point (°C)	–	–39	–39	GB/T 3535
Kinematic viscosity (40°C) mm^2/s	≤12	9.946	9.898	GB/T 265
Kinematic viscosity (0°C) mm^2/s	≤1800	54.46	54.58	
Kinematic viscosity (–10°C) mm^2/s	≤1800	102.0	101.6	
Kinematic viscosity (–20°C) mm^2/s	≤1800	206.8	207.6	
Moisture content (mg/kg)	≤30	17.0	6.0	GB/T 7600
Breakdown voltage (kV)	≥30	52.1	60.0	GB/T 507
Density (20°C) kg/m^3	≤895	832.4	832.6	SH/T 0604
Dielectric loss factor (90°C)	0.005	0.0007	0.0003	GB/T 5654
Acid value (mg KOH/g)	0.01	0.006	0.006	NB/SH/T 0836
Interfacial tension (mN/m)	≥40	49.1	50.3	GB/T 6541
Flash point (closed) (°C)	≥135	165	164	GB/T 261
Antioxidant content / (mass fraction %)	~0.08–0.40	0.30	0.30	SH/T 0792

https://doi.org/10.1007/s42860-022-00186-5 Published online by Cambridge University Press

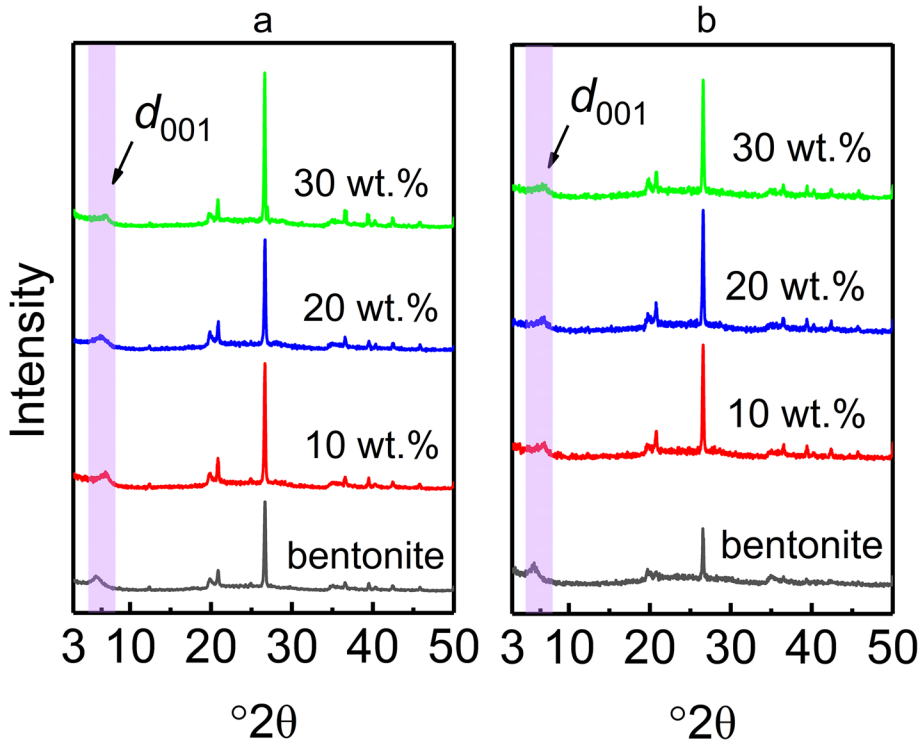

Fig. 8 XRD patterns of bentonite and bentonite modified with 10, 20, and 30 wt.% PAA-Na, **a** before and **b** after water adsorption for 12 h

according to the classification of IUPAC. The hysteresis loop indicated the presence of mesopores with the capillary condensation of liquid nitrogen on its surface (Gautier et al., 2010). The mesopores were stacked layer by layer (Korichi et al., 2009). Table 6 presents the results of surface area, total

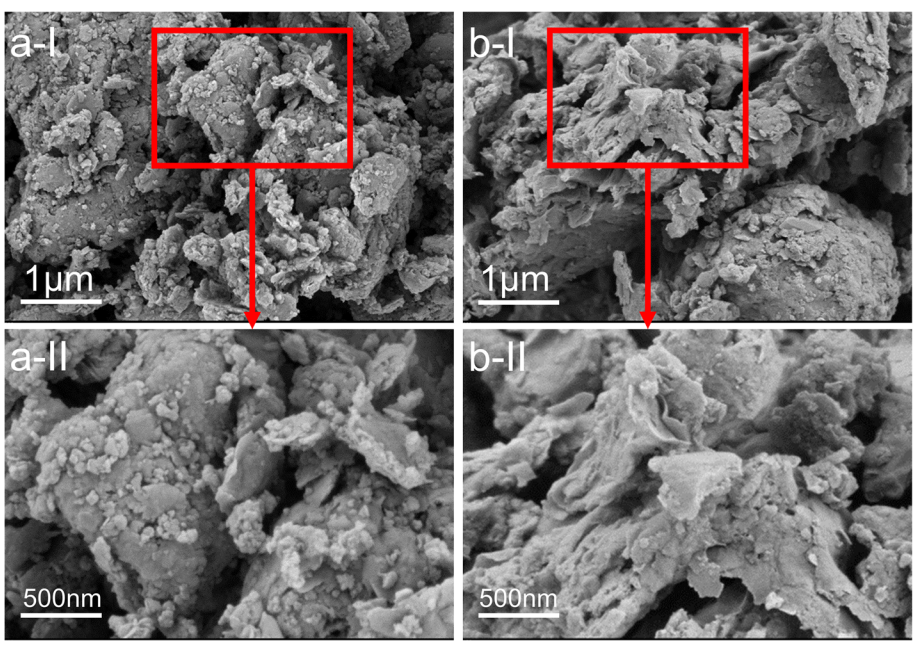

Fig. 9 SEM images of **a-I, II** bentonite and b-I, II bentonite modified with 20 wt.% PAA-Na

https://doi.org/10.1007/s42860-022-00186-5 Published online by Cambridge University Press

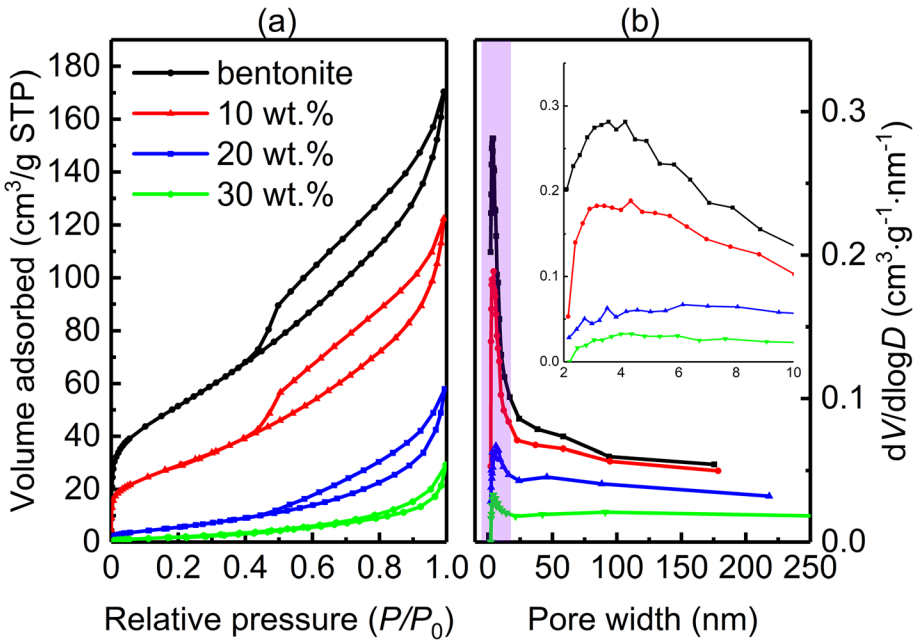

Fig. 10 Bentonite and bentonite modified with 10, 20, and 30 wt.% of PAA-Na: **a** N_2 adsorption-desorption isotherms and **b** pore-size distributions

pore volume, average pore diameter, and most frequent pore width for the bentonite and the modified bentonites. After modification, the surface area of the bentonites decreased from 168.2 to 5.0 m^2/g, the average pore diameter increased from 6.2 to 30.5 nm, and the pore volume decreased from 0.3 to 0.04 cm^3/g. The surface area and pore volume values for the modified bentonites were smaller than for bentonite; this may be due to the blockage of some of the finer pore junctions in the bentonite by the intercalation of the PAA-Na (Mahboub et al., 2006). These PAA-Na particles dispersed on the bentonite surface and in the pores. According to the results of dehydration and surface-area tests, the best dehydration effect of modified bentonite (20 wt.% PAA-Na) occurs because of the combination of pore adsorption in the bentonite and expansion of PAA-Na. When the amount of PAA-Na added was >20 wt.%, PAA-Na blocked the pore severely and reduced the water adsorption. The behavior of water adsorption changed with the addition of PAA-Na. The water-adsorption capacity of modified bentonite was increased with the addition of PAA-Na when it was <20 wt.%, due to the hydrophilicity of PAA-Na. Further addition of PAA-Na, on the other hand, blocked the pores and reduced the surface area of the bentonite, reducing its dehydration ability. The optimum addition of PAA-Na was found to be 20 wt.% (Fig. 3a), which balanced the benefits and drawbacks of the PAA-Na. The surface area and pore volume were reduced significantly, and the pore channels with smaller

Table 6 Textural properties of the investigated samples

Bentonite alone and with various amounts (wt.%) of PAA-Na added	Surface area (m^2/g)	Pore volume (cm^3/g)	Pore diameter (nm)	Most frequent pore width (nm)
Alone	168.2	0.3	6.2	3.6
10	92.9	0.2	8.0	4.3
20	23.4	0.1	14.5	6.1
30	5.0	0.04	30.5	4.4

https://doi.org/10.1007/s42860-022-00186-5 Published online by Cambridge University Press

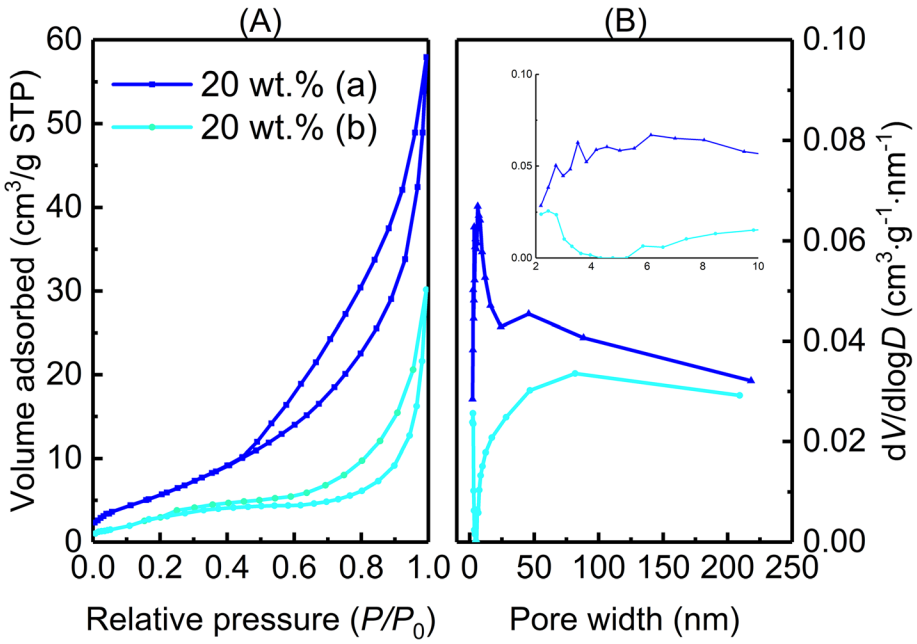

Fig. 11 Bentonite and bentonite modified with 20 wt% of PAA-Na: **A** N_2 adsorption-desorption isotherms (**a**) before and (**b**) after water adsorption; and **B** pore-size distributions **a** before and **b** after water adsorption

pore sizes were blocked by PAA-Na (Fig. 11). Only a few pores with relatively larger pore sizes remained (Table 7).

Broad Applicability of PAA-Na Modified Bentonite

The adsorption performance of various adsorbents in different oils varied, and the static adsorption capacity in different oils of several common adsorbents was demonstrated in Fig. 12. Different adsorbents were tested for 24 h under the conditions of 25°C, atmospheric pressure, and adsorbent:oil ratio of 1:20. PAA-Na modified bentonite had a high dehydration rate in xylene, naphtha, n-heptane, and diesel, indicating that its applicability is extremely wide.

Conclusions

The present work demonstrated a novel transformer oil dehydrant: PAA-Na modified bentonite. Compared with conventional adsorbents, it has a strong dehydration capacity in multiple oils and is suitable for many different oils. Both raw materials and processes are environmentally friendly. The pretreatment temperature was low (120°C). Moreover, the experimental space velocity operation is flexible, which is beneficial to industrial applications. FTIR spectra showed that PAA-Na had many hydrophilic groups. These hydrophilic groups are conducive to the capture of water molecules in oil. Morphology analysis showed PAA-Na was in an amorphous form. Thermal analysis indicated the thermal stability of PAA-Na modified bentonite could reach 200°C. The saturated water-vapor

Table 7 Textural properties of bentonite modified with 20 wt.% PAA-Na before (**a**) and after (**b**) water adsorption

Modified bentonite	Surface area (m^2/g)	Pore volume (cm^3/g)	Pore diameter (nm)	Most frequent pore width (nm)
(a)	23.4	0.1	14.5	6.1
(b)	6.4	0.04	26.6	81.7

https://doi.org/10.1007/s42860-022-00186-5 Published online by Cambridge University Press

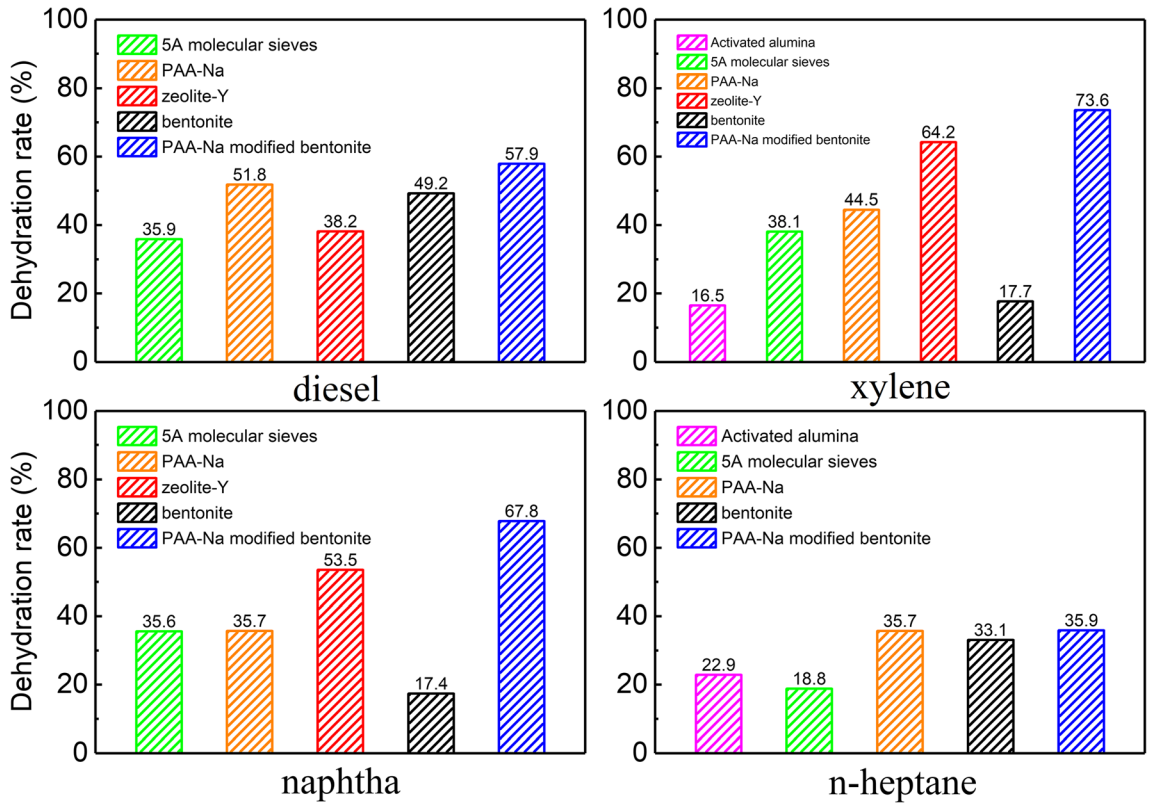

Fig. 12 Static adsorption capacities of various adsorbents and bentonite modified with 20 wt.% PAA-Na for various oils

adsorption studies indicated that the adsorption equilibrium could be well described by the Freundlich model. This work focused on the formulation of bentonite modified with PAA-Na and determined that the optimum material mix ratio was 20 wt.% PAA-Na in bentonite.

Acknowledgments The authors acknowledge funding from the National Natural Science Foundation of China (Grant No. 21808054).

Authors' contributions Naiwang Liu contributed to the conception of the study; Li Shi and Xuan Meng helped perform the analysis with constructive discussions. Li Shi and Xuan Meng provided constructive suggestions for the revision of the manuscript, including the fitting of adsorption isotherms and the analysis of in situ IR.

Fanyu Meng performed the experiment, contributed significantly to analysis and manuscript preparation, performed the data analyses, and wrote the manuscript.

Funding This study was supported in part by grants from the national natural science foundation of China (No.21808054).

Declarations

Conflicts of interest There are no conflicts to declare.

Ethics approval and Consent to participate No animal or human testing is covered in this paper.

Data availability All data generated or analyzed during this study are included in this article.

Consent for publication Not applicable

References

Becher, T. B., Braga, C. B., Bertuzzi, D. L., Ramos, M. D., Hassan, A., Crespilho, F. N., & Ornelas, C. (2019). The structure-property relationship in LAPONITE(R) materials: from Wigner glasses to strong self-healing hydrogels formed by non-covalent interactions. *Soft Matter, 15*(6), 1278–1289. https://doi.org/10.1039/c8sm01965g

Dechambre, D., Thien, J., & Bardow, A. (2017). When 2nd generation biofuel meets water – The water solubility and phase stability issue. *Fuel, 209*, 615–623. https://doi.org/10.1016/j.fuel.2017.07.110

Frink, L. A., & Armstrong, D. W. (2016). Determination of Trace Water Content in Petroleum and Petroleum Products. *Analytical Chemistry, 88*(16), 8194–8201. https://doi.org/10.1021/acs.analchem.6b02006

Gautier, M., Muller, F., Le Forestier, L., Beny, J. M., & Guegan, R. (2010). NH_4-smectite: Characterization, hydration properties and hydro mechanical behaviour. *Applied Clay Science, 49*(3), 247–254. https://doi.org/10.1016/j.clay.2010.05.013

Ghosal, P. S., & Gupta, A. K. (2015). An insight into thermodynamics of adsorptive removal of fluoride by calcined Ca–Al–(NO_3) layered double hydroxide. *RSC Advances, 5*(128), 105889–105900. https://doi.org/10.1039/c5ra20538g

Guerra, S. R., Merat, L. M. O. C., San Gil, R. A. S., & Dieguez, L. C. (2008). Alkylation of benzene with olefins in the presence of zirconium-pillared clays. *Catalysis Today, 133-135*, 223–230. https://doi.org/10.1016/j.cattod.2007.12.094

Horváth, G., & Kawazoe, K. (1983). Method for the calculation of effective pore size distribution in molecular sieve carbon. *Journal of Chemical Engineering of Japan, 16*(6), 470–475.

Kaufhold, S., Dohrmann, R., & Klinkenberg, M. (2010). Water-Uptake Capacity of Bentonites. *Clays and Clay Minerals, 58*(1), 37–43. https://doi.org/10.1346/ccmn.2010.0580103

Kawi, S., & Yao, Y. Z. (1999). Silica bonded K10 montmorillonite (SBM): a high surface area catalytic clay material. *Microporous and Mesoporous Materials, 28*(1), 25–34. https://doi.org/10.1016/s1387-1811(98)00279-0

Korichi, S., Elias, A., & Mefti, A. (2009). Characterization of smectite after acid activation with microwave irradiation. *Applied Clay Science, 42*(3-4), 432–438.

Lam, J. K. W., Hetherington, J. I., & Carpenter, M. D. (2013). Ice growth in aviation jet fuel. *Fuel, 113*, 402–406. https://doi.org/10.1016/j.fuel.2013.05.048

Li, C., Wu, Q., Petit, S., Gates, W. P., Yang, H., Yu, W., & Zhou, C. (2019). Insights into the Rheological Behavior of Aqueous Dispersions of Synthetic Saponite: Effects of Saponite Composition and Sodium Polyacrylate. *Langmuir, 35*(40), 13040–13052. https://doi.org/10.1021/acs.langmuir.9b01805

Liu, Y., Huang, G., Pan, Z., Wang, Y., & Li, G. (2021). Synthesis of sodium polyacrylate copolymers as water-based dispersants for wet ultrafine grinding of cobalt aluminate particles. *Colloids and Surfaces A: Physicochemical and Engineering Aspects, 610*, 125553.

Mahboub, R., Mouzdahir, Y. E., Elmchaouri, A., Carvalho, A., Pinto, M., & Pires, J. (2006). Characterization of a delaminated clay and pillared clays by adsorption of probe molecules. *Colloids and Surfaces A: Physicochemical and Engineering Aspects, 280*(1-3), 81–87. https://doi.org/10.1016/j.colsurfa.2006.01.036

Moussa, O., Tarlet, D., Massoli, P., & Bellettre, J. (2018). Parametric study of the micro-explosion occurrence of W/O emulsions. *International Journal of Thermal Sciences, 133*, 90–97. https://doi.org/10.1016/j.ijthermalsci.2018.07.016

Murray, H. H. (2006). Chapter 6 Bentonite Applications. In *Applied Clay Mineralogy - Occurrences, Processing and Application of Kaolins, Bentonites, Palygorskite-Sepiolite, and Common Clays* (pp. 111-130). https://doi.org/10.1016/s1572-4352(06)02006-x

Narayan, S., Moravec, D. B., Hauser, B. G., Dallas, A. J., & Dutcher, C. S. (2018). Removing Water from Diesel Fuel: Understanding the Impact of Droplet Size on Dynamic Interfacial Tension of Water-in-Fuel Emulsions. *Energy & Fuels, 32*(7), 7326–7337. https://doi.org/10.1021/acs.energyfuels.8b00502

Natkański, P., Kuśtrowski, P., Białas, A., Piwowarska, Z., & Michalik, M. (2012). Controlled swelling and adsorption properties of polyacrylate/montmorillonite composites. *Materials Chemistry and Physics, 136*(2-3), 1109–1115. https://doi.org/10.1016/j.matchemphys.2012.08.061

Park, Y., Ayoko, G. A., & Frost, R. L. (2011). Characterisation of organoclays and adsorption of p-nitrophenol: environmental application. *Journal of Colloid and Interface Science, 360*(2), 440–456. https://doi.org/10.1016/j.jcis.2011.04.085

Powers, M. L. (1990). Analysis of Gravity Separation in Freewater Knockouts. *SPE Production Engineering, 5*(1), 52–58.

Prakoso, M. H. (2015). Effects of water content on dielectric properties of mineral transformer oil. *International Journal of Electrical and Computer Engineering, 9*(10), 1142–1146.

Saleem, M., Afzal, M., Qadeer, R., & Hanif, J. (1992). Selective adsorption of uranium on activated charcoal from electrolytic aqueous solutions. *Separation Science, 27*(2), 239–253.

Santiago, F., Mucientes, A. E., Osorio, M., & Rivera, C. (2007). Preparation of composites and nanocomposites based on bentonite and poly(sodium acrylate). Effect of amount of bentonite on the swelling behaviour. *European Polymer Journal, 43*(1), 1–9. https://doi.org/10.1016/j.eurpolymj.2006.07.023

Saththasivam, J., Loganathan, K., & Sarp, S. (2016). An overview of oil-water separation using gas flotation systems. *Chemosphere, 144*, 671–680. https://doi.org/10.1016/j.chemosphere.2015.08.087

Seaton, N. A., Walton, J., & Quirke, N. (1989). A new analysis method for the determination of the pore size distribution of porous carbons from nitrogen adsorption measurements. *Carbon, 27*(6), 853–861.

Sheng, H., Welker, J., & Sliepcevich, C. (1974). Liquid-liquid separations in a conventional hydrocyclone. *The Canadian Journal of Chemical Engineering, 52*(4), 487–491.

Spielman, L. A., & Goren, S. L. (1970). Progress in induced coalescence and a new theoretical framework for coalescence by porous media. *Industrial & Engineering Chemistry, 62*(10), 10–24.

Takeno, H., & Nagai, S. (2018). Mechanical Properties and Structures of Clay-Polyelectrolyte Blend Hydrogels. *Gels, 4*(3). https://doi.org/10.3390/gels4030071

Takeno, H., & Nakamura, A. (2019). Effects of molecular mass of polymer on mechanical properties of clay/poly (ethylene oxide) blend hydrogels, and comparison between them and clay/sodium polyacrylate blend hydrogels. *Colloid and Polymer Science, 297*(4), 641–649. https://doi.org/10.1007/s00396-019-04476-8

Teo, W. K., & Ruthven, D. M. (1986). Adsorption of water from aqueous ethanol using 3-. ANG. molecular sieves. *Industrial & Engineering Chemistry Process Design and Development, 25*(1), 17–21.

Xu, H., Liu, J., Wang, Y., Cheng, G., Deng, X., & Li, X. (2014). Oil removing efficiency in oil–water separation flotation column. *Desalination and Water Treatment, 53*(9), 2456–2463. https://doi.org/10.1080/19443994.2014.908413

Ye, G., Breugel, K. V., Lura, P., & Mechtcherine, V. (2012). *Application of Super Absorbent Polymers (SAP) in Concrete Construction* (pp. 13–15). Springer, Dordrecht, The Netherlands. https://doi.org/10.1007/978-94-007-2733-5

Yu, C., Liao, R., Cai, X., & Yu, X. (2019). Sodium polyacrylate modification method to improve the permeant performance of bentonite in chemical resistance. *Journal of Cleaner Production, 213*, 242–250. https://doi.org/10.1016/j.jclepro.2018.12.179